

EFFECTS OF BROWNIAN MOTION AND THERMOPHORESIS VARIATION ON MHD NANOFLUID FLOW IN A CONCENTRATED PARABOLIC THERMAL SOLAR COLLECTOR

¹Lucas Khaoya Mukwabi, ²Dr. Mark Kimathi, ³Dr. Charles Muli

Department of Mathematics, Machakos University,
P.O Box 136 - 90100, Machakos, Kenya.

DOI: <https://doi.org/10.5281/zenodo.7804696>

Published Date: 06-April-2023

Abstract: This research paper investigates the effects of Thermophoresis and Brownian motion parameter variation on heat and mass transfer on MHD nanofluid flow in a parabolic thermal solar collector. The effect of laminar flow which is occasioned by a variation in the Brownian motion and Thermophoresis parameter over a parabolic shaped photovoltaic surface has been investigated numerically. The model used for the nanofluid flow incorporates the effects of Brownian motion and thermophoresis parameter variation with thermal variation due to solar radiation in the presence of an induced magnetic field cutting perpendicular across the flow. The governing equations of the MHD fluid flow are presented and solved using the finite element method. The results show that increasing the Thermophoresis (Nt) and Brownian motion parameters (Nb) lead to an increase in heat transfer and a decrease in mass transfer. Similarly, an increase in the Peclet number (Pe) favors mass transfer but impairs heat transfer. A comparison of the results with existing literature has been done and a remarkable agreement established.

Keywords: Brownian Motion, Concentration Boundary Layer, Heat Transfer, Mass Transfer, Magneto-Hydrodynamics (MHD), Nanofluid, Photovoltaic Solar Collector, Thermal Boundary Layer, Thermophoresis, Velocity Boundary Layer.

1. INTRODUCTION

1.1 Background Information

The desire for high-performance heat transfer fluid has been a subject of numerous scientific researches over the years. Due to metals having a higher conductivity as compared to fluids, most researchers have focused their studies on the thermal behavior of solid particles suspended in liquids to enhance the base fluid conductivity. The main idea was to develop a solid-fluid suspension mixture with more excellent heat conductivity than conventional heat transfer fluids such as water.

Such advancement has resulted in the development of nanofluids. Nanofluids are colloidal suspensions made out of nanoparticles of less than 100nm in diameter dispersed in a base fluid and having a bulk solid thermal conductivity higher than that of the base fluid. Nanofluids have been extensively used to improve heat transfer and energy efficiency in many thermal control systems. One key area that has equally not been left out is solar panel manufacturing.

Solar energy is one of the most secure, reliable and environmentally-friendly forms of renewable energy. [1] Among the widely dependable and exploited forms of renewable energy, solar energy is considered a better form of energy compared to fossil fuels since it is clean as it offers minimal adverse environmental effects. Thermal solar collectors are very popular and adopted globally to collect and convert solar energy into thermal energy. The adoption of solar power plays a vital role in providing clean energy and reducing global warming.

The in-cooperation of nanofluids in thermal solar collectors as the working fluid is vital in achieving a higher probability of thermal harnessing with the least probable concentrations. [2] The potential advantage of using nanofluids as a working fluid in thermal solar collectors ranges from a) higher thermal conductivities b) excellent stability and c) low wear and tear due to an increase in pressure drop and pipe wall abrasion experienced as a result of the suspension of nanoparticles. The use of nanofluids as the working fluid in the solar collector is essential in achieving green and clean energy.

In recent years, the study of magneto-hydrodynamics (MHD) fluid flow has become increasingly important due to its wide range of applications in various engineering fields [3, 4, 5, and 6]. MHD flow is influenced by various factors such as magnetic field, thermophoresis, Brownian motion, etc. In the present study, we considered the combined effects of Brownian motion and thermophoresis parameter variation in the presence of thermal stratification due to solar radiation on heat and mass transfer of MHD fluid in a parabolic thermal solar collector.

1.2 Definitions of Terms

1.2.1 Thermophoresis

Thermophoresis is the phenomenon where particles or molecules in a fluid move in response to a temperature gradient. The magnitude and direction of thermophoresis flow depends on the properties of the fluid and the suspended particles, as well as the temperature gradient.

1.2.2 Brownian Motion.

Brownian motion is the random motion of particles suspended in a fluid or gas, caused by the thermal motion of the surrounding molecules. The motion of particles in Brownian motion is the result of the random collisions between the suspended particles and the surrounding fluid molecules.

1.2.3 Heat and Mass Transfer.

Heat and mass transfer in fluid flow refers to the transfer of thermal energy and matter between a fluid and its surroundings. In fluid flow, heat transfer occurs due to the temperature difference between the fluid and the surrounding environment, while mass transfer occurs due to the concentration difference of a particular species in the fluid and the surrounding environment.

1.2.4 Magneto-hydrodynamics (MHD)

Magneto-hydrodynamics (MHD) is a field of physics and engineering that studies the dynamics of electrically conducting fluids in the presence of magnetic fields. The term "magneto-hydrodynamics" refers to the coupling between the magnetic and hydrodynamic (fluid flow) phenomena in such systems.

2. MATHEMATICAL FORMULATION

The present study considers the unsteady flow of graphene-water nanofluid through the receiver tube of a parabolic thermal solar collector under the influence of a strong induced magnetic field b that cuts perpendicular to the flow direction. For a parabolic surface flow, the velocity profile is assumed to be laminar and parabolic in shape, with the maximum velocity occurring at the centerline of the surface. An unsteady cylindrical coordinate system (r, z, t) is chosen such that the z -direction is along the axis of the receiver tube while the r -direction is normal to the flow field. The flow of the nanofluid is along the z -dimension, thus velocity is along the z -direction while the velocity varies along the r -direction from the no-slip boundary and is maximum at the free stream. The nanofluid is considered a grey diffuse emitter and reflector of radiation heat flux. Boussinesq approximation is used to include the gravitational acceleration to the opposite of the radial direction.

2.1 Specific Governing Equations.

The flow of a thermally incited nanofluid is theoretically described by the continuity, momentum, and energy equations [2]. The governing equations are modified to perfectly suit a particular fluid flow under review. The laws on which the final working is based on are determined by the specific assumptions by which the simplified form of the equations are obtained.

2.1.1 Continuity Equation.

The continuity equation is derived from the principle of mass conservation which states that under normal conditions, mass is neither created nor destroyed. In fluid flow simulation, regardless of the system of fluid particles chosen, the identity of the particles remains the same by definition of the system and thus the mass of the entire system remains constant. The flow of any fluid is possible only if the continuity equation is satisfied. Mathematically, the specific continuity equation in the present study is expressed as:

$$\frac{\partial u_r}{\partial r} + \frac{u_r}{r} + \frac{\partial u_z}{\partial z} = 0 \quad (1)$$

2.1.2 Momentum Equations.

The momentum equation is a fundamental equation in fluid mechanics that describes the changes in the fluid velocity in response to the forces acting on it. The momentum of a body is expressed as the product of its mass and velocity. In the present study, the Lorentz force that describes the MHD phenomenon and buoyancy force that accounts for variance in density with temperature and concentration are considered. For fluid flow, the rate of change of linear momentum of a fluid mass flux is equal to the external force acting on it. The mathematical representation of the momentum equations both on the axial and radial direction of the flow are specifically expressed as;

r -Momentum Equation

$$\begin{aligned} \rho_{nf} \left[\frac{\partial u_r}{\partial t} + u_r \frac{\partial u_r}{\partial r} + u_z \frac{\partial u_r}{\partial z} \right] = & -\frac{\partial P}{\partial r} + \mu_{nf} \left(\frac{\partial^2 u_r}{\partial r^2} + \frac{1}{r} \frac{\partial u_r}{\partial r} + \frac{\partial^2 u_r}{\partial z^2} \right) \\ & + \rho_{nf} (\beta_T)_{nf} (T - T_\infty) + \rho_{nf} (\beta_C)_{nf} (C - C_\infty) \\ & - B_o^2 u_r \sigma_{nf} \end{aligned} \quad (2)$$

z - Momentum Equation.

$$\begin{aligned} \rho_{nf} \left[\frac{\partial u_z}{\partial t} + u_r \frac{\partial u_z}{\partial r} + u_z \frac{\partial u_z}{\partial z} \right] = & -\frac{\partial P}{\partial z} + \mu_{nf} \left(\frac{\partial^2 u_z}{\partial r^2} + \frac{1}{r} \frac{\partial u_z}{\partial r} + \frac{\partial^2 u_z}{\partial z^2} \right) + \rho_{nf} (\beta_T)_{nf} (T - T_\infty) \\ & + \rho_{nf} (\beta_C)_{nf} (C - C_\infty) - (B_o^2 u_z + b^2 u_z) \end{aligned} \quad (3)$$

2.1.3 Energy Equation.

Also referred as the first law of thermodynamics. The energy equation is derived from the principle of energy conservation, which states that the amount of heat energy added to a system is equal to the resultant change in internal energy and work done within the system. In the present study, thermal radiation and Joules heating were considered as the energy source terms. Mathematically, the specific energy equation under review is expressed as:

$$\begin{aligned}
 (\rho C_P)_{nf} \left[\frac{\partial T}{\partial t} + u_r \frac{\partial T}{\partial r} + u_z \frac{\partial T}{\partial z} \right] &= \kappa_{nf} \left[\frac{\partial^2 T}{\partial r^2} + \frac{1}{r} \frac{\partial T}{\partial r} + \frac{\partial^2 T}{\partial z^2} \right] + \frac{16\sigma^* T_\infty^3}{3k^*} \frac{\partial^2 T}{\partial r^2} + \sigma_{nf} (B_0 u_r)^2 \\
 &+ (\rho C_p) \left[D_B \left(\frac{\partial C}{\partial r} \frac{\partial T}{\partial r} + \frac{\partial C}{\partial z} \frac{\partial T}{\partial z} \right) + \frac{D_T}{T_\infty} \left[\left(\frac{\partial T}{\partial r} \right)^2 + \left(\frac{\partial T}{\partial z} \right)^2 \right] \right]
 \end{aligned} \tag{4}$$

2.1.4 Species Concentration Equation.

The species concentration equation also referred to as the advection-diffusion equation. It is a fundamental equation in fluid mechanics that describes the transport of chemical species in a fluid. The equation is derived from the principle of conservation of mass and takes into account the effect of advection that is due to the transport of substance due to a bulk motion of the fluid and diffusion which is the transport of the substance due to random molecular motion. In this study, thermophoresis which is the mass flux generated by the existence of temperature and nanoparticle concentration gradient in the nanofluid is considered as the species source term. Mathematically, the specific species concentration equation under review is expressed as:

$$\frac{\partial C}{\partial t} + u_r \frac{\partial C}{\partial r} + u_z \frac{\partial C}{\partial z} = D_B \left[\frac{\partial^2 C}{\partial r^2} + \frac{1}{r} \frac{\partial C}{\partial r} + \frac{\partial^2 C}{\partial z^2} \right] + \frac{D_T}{T_\infty} \left[\frac{\partial^2 T}{\partial r^2} + \frac{1}{r} \frac{\partial T}{\partial r} + \frac{\partial^2 T}{\partial z^2} \right] \tag{5}$$

2.1.5 Magnetic Induction Equation.

The magnetic induction equation is a fundamental equation in Magnetohydrodynamics that describes the behavior of an electrically conducting fluid in presence of a magnetic field. In fluid mechanics, the magnetic induction equation describes how the magnetic field changes over time. The magnetic induction equation accounts for the induced magnetic field in the present study. Mathematically, the specific magnetic induction equation under review is expressed as:

$$\frac{\partial b}{\partial t} = b \frac{\partial u_r}{\partial z} + D_m \left[\frac{\partial^2 b}{\partial r^2} + \frac{1}{r} \frac{\partial b}{\partial r} + \frac{\partial^2 b}{\partial z^2} \right] \tag{6}$$

2.1.6 Boundary Conditions.

The initial and final systems of equations are subjected to Dirichlet and Neumann boundary conditions and incorporate the slip boundary conditions.

$$\frac{\partial u_r}{\partial r} = 0, \frac{\partial u_z}{\partial r} = 0, \frac{\partial T}{\partial r} = 0, \frac{\partial C}{\partial r} = 0 \quad \text{At } r=0 \text{ (centerline)}$$

$$u_r = 0, u_z = 0, T = T_{wall}, C = C_{wall} \quad \text{At } r=a \text{ (wall)}$$

$$u_r = 0, u_z = 0, T = T_\infty, C = C_\infty \quad \text{At } z=0 \text{ (inlet)}$$

(7)

$$\frac{\partial u_r}{\partial z} = 0, \frac{\partial u_z}{\partial z} = 0, \frac{\partial T}{\partial z} = 0, \frac{\partial C}{\partial z} = 0 \quad \text{At } z=L \text{ (outlet)}$$

$$u_r = 0, u_z = 0, T = T_\infty, C = C_\infty \quad \text{At } t=0 \text{ (initial conditions)}$$

3. NON-DIMENSIONALIZATION OF THE GOVERNING EQUATIONS

The governing partial differential equations 1,2,3,4,5 and 6 together with their boundary conditions expressed by equation 7 above are transformed into a system of ordinary differential equations by employing a system of non-dimensional numbers then solved numerically by employing the finite element method. The study represents dimensional variables with the superscript (*) star basing the non-dimensionalization on the scaling variables listed below;

$$r^* = \frac{r}{L}, z^* = \frac{z}{L}, t^* = \frac{tu_\infty}{L}, b^* = \frac{b}{B}, \phi = \frac{C - C_\infty}{C_w - C_\infty}, \theta = \frac{T - T_\infty}{T_w - T_\infty},$$

$$p^* = \frac{p}{\rho u_\infty}, u_r^* = \frac{u_r}{u_\infty}, u_z^* = \frac{u_z}{u_\infty} \tag{8}$$

Using the non-dimensional numbers expressed by equation (8) above, the governing equations are thus reduced to;

$$d_1 \left[\frac{\partial u_r^*}{\partial t^*} + u_r^* \frac{\partial u_r^*}{\partial r^*} + u_z^* \frac{\partial u_r^*}{\partial z^*} \right] = -\frac{dP^*}{dr^*} + \frac{d_4}{Re} \left(\frac{\partial^2 u_r^*}{\partial r^{*2}} + \frac{1}{r^*} \frac{\partial u_r^*}{\partial r^*} + \frac{\partial^2 u_r^*}{\partial z^{*2}} \right)$$

$$+ d_1 Gr_T \theta + d_1 Gr_C \phi - d_2 M^2 u_r^* \tag{9}$$

$$d_1 \left[\frac{\partial u_z^*}{\partial t^*} + u_z^* \frac{\partial u_z^*}{\partial z^*} \right] = \frac{d_4}{Re} \left(\frac{\partial^2 u_z^*}{\partial z^{*2}} \right) + d_1 Gr_T \theta + d_1 Gr_C \phi + d_2 M^2 (1 - b^{*2}) \tag{10}$$

$$d_3 \left[\frac{\partial \theta}{\partial t^*} + u_r^* \frac{\partial \theta}{\partial r^*} + u_z^* \frac{\partial \theta}{\partial z^*} \right] = \frac{d_5}{Pe} \left[\left(\frac{\partial^2 \theta}{\partial r^{*2}} + \frac{1}{r^*} \frac{\partial \theta}{\partial r^*} + \frac{\partial^2 \theta}{\partial z^{*2}} \right) \right] + \frac{Rd}{Pe} \frac{\partial^2 \theta}{\partial r^{*2}} + d_4 u_r^{*2} M^2 Ec$$

$$+ d_3 Nb \left(\frac{\partial \phi}{\partial r^*} \frac{\partial \theta}{\partial r^*} + \frac{\partial \phi}{\partial z^*} \frac{\partial \theta}{\partial z^*} \right) + Nt \left(\frac{\partial^2 \theta}{\partial r^{*2}} + \frac{\partial^2 \theta}{\partial z^{*2}} \right) \tag{11}$$

$$\frac{\partial \phi}{\partial t^*} + u_r^* \frac{\partial \phi}{\partial r^*} + u_z^* \frac{\partial \phi}{\partial z^*} = \frac{1}{Sc} \cdot \frac{1}{Re} \left[\frac{\partial^2 \phi}{\partial r^{*2}} + \frac{1}{r^*} \frac{\partial \phi}{\partial r^*} + \frac{\partial^2 \phi}{\partial z^{*2}} \right] +$$

$$\frac{Nt}{Nb} \cdot \frac{1}{Sc} \cdot \frac{1}{Re} \left[\frac{\partial^2 \theta}{\partial r^{*2}} + \frac{1}{r^*} \frac{\partial \theta}{\partial r^*} + \frac{\partial^2 \theta}{\partial z^{*2}} \right] \tag{12}$$

$$\frac{\partial b^*}{\partial t^*} = b^* \frac{\partial u_r^*}{\partial z^*} + \frac{1}{Rm} \left[\frac{\partial^2 b^*}{\partial r^{*2}} + \frac{1}{r^*} \frac{\partial b^*}{\partial r^*} + \frac{\partial^2 b^*}{\partial z^{*2}} \right] \tag{13}$$

Equations 9 to 13 above are the dimensionless forms for the momentum, energy, species concentration and magnetic induction equations. The coefficient d1, d2, d3, d4 and d5 are used to express the thermo-physical relationship between the nanoparticle, base fluid and the nanofluid as expressed below;

$$\begin{aligned}
 d_1 &= \frac{\rho_{nf}}{\rho_f} = \left[(1 - \phi) + \left(\frac{\rho_s}{\rho_f} \right) \phi \right] \\
 d_2 &= \frac{\sigma_{nf}}{\sigma_f} = \left[1 + \frac{3(\phi - 1)\phi}{(\phi + 2) - (\phi - 1)\phi} \right] \\
 d_3 &= \frac{(\rho C_p)_{nf}}{(\rho C_p)_f} = \left[(\phi - 1) + \phi \frac{(\rho C_p)_s}{(\rho C_p)_f} \right] \\
 d_4 &= \frac{\mu_{nf}}{\mu_f} = \frac{1}{(1 - \phi)^{2.5}} \\
 d_5 &= \frac{\kappa_{nf}}{\kappa_f} = \left[\frac{\kappa_{nf} + 2\kappa_f - 2\phi(\kappa_f - \kappa_{nf})}{\kappa_{nf} + 2\kappa_f + 2\phi(\kappa_f - \kappa_{nf})} \right] \tag{14}
 \end{aligned}$$

Similarly, the boundary conditions expressed by equation (7) above are dimensionalized using the non – dimensional numbers to give;

$$\begin{aligned}
 \frac{\partial u_r^*}{\partial r^*} = 0, \frac{\partial u_z^*}{\partial r^*} = 0, b = B_0 b^*, \frac{\partial \theta}{\partial r^*} = 0, \frac{\partial \phi}{\partial r^*} = 0 & \quad \text{At } r = 0 \\
 u_r^* = 0, u_z^* = 0, b^* = 0, \theta = 1, \phi = 1 & \quad \text{At } r = a \\
 u_r^* = 0, u_z^* = 0, b^* = 1, \theta = 0, \phi = 0 & \quad \text{At } z = 0 \\
 u_r^* = 0, u_z^* = 0, b^* = 0, \theta = 0, \phi = 0 & \quad \text{At } t = 0
 \end{aligned} \tag{15}$$

4. NUMERICAL SOLUTIONS

The governing equations that describe the flow, heat and mass transfer equations of the model under review are coupled and highly nonlinear. Hence, the system together with the boundary conditions is evaluated numerically using the finite difference technique. The discretization is accomplished by incorporating forward and central difference approximations respectively to first and second order partial derivatives. The domain of the problem is discretized into discrete points that constitute the mesh for the problem. The relationship between the partial derivatives in the differential equations and the function values at adjacent nodal points are expressed in a uniform mesh by taking the *r – z* plane and dividing it into a network of uniform rectangular cells with width Δz and height Δr with *j* and *i* referring to *z* and *r* respectively. The Δz represents a stepwise change in the *z – direction* while Δr represents a stepwise change in the *r – direction*. A spatial change in the *r – direction* is expressed as $r = i\Delta r$ while a spatial change in the *z – direction* is expressed as $z = j\Delta z$. Using the Taylor series expansion of the dependent variable about a grid point (i, j) , the stencils for the governing equations are expressed as;

$$\begin{aligned}
 & d_1 * \left[\left(\frac{U_{i,j}^{k+1} - U_{i,j}^k}{\Delta t} \right) + (U_{i,j}^k) * \left(\frac{U_{i+1,j}^k - U_{i-1,j}^k}{2\Delta r} \right) + (V_{i,j}^k) * \left(\frac{V_{i,j+1}^k - V_{i,j-1}^k}{2\Delta z} \right) \right] \\
 & = \left(\frac{P_{i+1,j}^k - P_{i-1,j}^k}{2\Delta r} \right) + \frac{d_4}{\text{Re}} * \left[\left(\frac{U_{i+1,j}^k - 2U_{i,j}^k + U_{i-1,j}^k}{(\Delta r)^2} \right) + \left(\frac{1}{r_{i,j}} \right) * \left(\frac{U_{i+1,j}^k - U_{i-1,j}^k}{2\Delta r} \right) \right] \tag{16} \\
 & + \left(\frac{V_{i,j+1}^k - 2V_{i,j}^k + V_{i,j-1}^k}{(\Delta z)^2} \right) + d_1 * Gr_T * \theta_{i,j}^k + d_1 * Gr_C * \phi_{i,j}^k + d_4 * M * M * (U_{i,j}^k)
 \end{aligned}$$

$$\begin{aligned}
 d_1 * \left[\left(\frac{V_{i,j}^{k+1} - V_{i,j}^k}{\Delta t} \right) + (U_z) * \left(\frac{V_{i,j+1}^k - V_{i,j-1}^k}{2\Delta z} \right) \right] & = \frac{d_4}{\text{Re}} * \left(\frac{V_{i,j+1}^k - 2V_{i,j}^k + V_{i,j-1}^k}{(\Delta z)^2} \right) + d_1 * Gr_T * \theta \\
 & + d_1 * Gr_C * \phi_{i,j}^k + d_2 * M * M * (1 - b_{i,j}^k * b_{i,j}^k) \tag{17}
 \end{aligned}$$

$$\begin{aligned}
 & d_3 * \left[\frac{\theta_{i,j}^{k+1} - \theta_{i,j}^k}{\Delta t} + (U_{i,j}^k) * \left(\frac{\theta_{i+1,j}^k - \theta_{i-1,j}^k}{2\Delta r} \right) + (V_{i,j}^k) * \left(\frac{\theta_{i,j+1}^k - \theta_{i,j-1}^k}{2\Delta z} \right) \right] \\
 & = \frac{d_5}{\text{Pe}} * \left[\left(\frac{\theta_{i+1,j}^k - 2\theta_{i,j}^k + \theta_{i-1,j}^k}{(\Delta r)^2} \right) + \left(\frac{1}{r_{i,j}^k} \right) * \left(\frac{\theta_{i+1,j}^k - \theta_{i-1,j}^k}{2\Delta r} \right) \right]
 \end{aligned}$$

$$+ \left(\frac{\theta_{i,j+1}^k - 2\theta_{i,j}^k + \theta_{i,j-1}^k}{(\Delta z)^2} \right) + \frac{Rd}{\text{Pe}} \left[\left(\frac{\theta_{i+1,j}^k - 2\theta_{i,j}^k + \theta_{i,j-1}^k}{(\Delta r)^2} \right) + \right]$$

$$d_4 * (U_{i,j}^k) * M * M * Ec + d_3 * Nb * \left[\left(\frac{\phi_{i+1,j}^k - \phi_{i-1,j}^k}{2\Delta r} \right) * \left(\frac{\theta_{i+1,j}^k - \theta_{i-1,j}^k}{2\Delta r} \right) \right]$$

$$+ \left(\frac{\phi_{i,j+1}^k - \phi_{i,j-1}^k}{2\Delta z} \right) * \left(\frac{\theta_{i,j+1}^k - \theta_{i,j-1}^k}{2\Delta z} \right) + Nt \left[\left(\frac{\theta_{i+1,j}^k - 2\theta_{i,j}^k + \theta_{i-1,j}^k}{(\Delta r)^2} \right) \right] \tag{18}$$

$$+ \left(\frac{\theta_{i,j+1}^k - 2\theta_{i,j}^k + \theta_{i,j-1}^k}{(\Delta z)^2} \right)$$

$$\begin{aligned} & \frac{\phi_{i,j}^{k+1} - \phi_{i,j}^k}{\Delta t} + \left(U_{i,j}^k \right) * \left(\frac{\phi_{i+1,j}^k - \phi_{i-1,j}^k}{2\Delta r} \right) + \left(V_{i,j}^k \right) * \left(\frac{\phi_{i,j+1}^k - \phi_{i,j-1}^k}{2\Delta z} \right) \\ &= \frac{1}{Sc} * \frac{1}{Re} * \left[\left(\frac{\phi_{i+1,j}^k - 2\phi_{i,j}^k + \phi_{i-1,j}^k}{(\Delta r)^2} \right) + \left(\frac{1}{r_{i,j}^k} \right) * \left(\frac{\phi_{i+1,j}^k - \phi_{i-1,j}^k}{2\Delta r} \right) \right. \\ & \left. + \left(\frac{\phi_{i,j+1}^k - 2\phi_{i,j}^k + \phi_{i,j-1}^k}{(\Delta z)^2} \right) \right] + \frac{1}{Sc} * \frac{1}{Re} * \frac{Nt}{Nb} \left[\left(\frac{\phi_{i+1,j}^k - 2\phi_{i,j}^k + \phi_{i-1,j}^k}{(\Delta r)^2} \right) + \right. \\ & \left. \left(\frac{1}{r_{i,j}^k} \right) * \left(\frac{\phi_{i+1,j}^k - \phi_{i-1,j}^k}{2\Delta r} \right) + \left(\frac{\phi_{i,j+1}^k - 2\phi_{i,j}^k + \phi_{i,j-1}^k}{(\Delta z)^2} \right) \right] \end{aligned} \tag{19}$$

$$\begin{aligned} & \frac{b_{i,j}^{k+1} - b_{i,j}^k}{\Delta t} = \left(b_{i,j}^k \right) * \left(\frac{b_{i,j+1}^k - b_{i,j-1}^k}{2\Delta z} \right) + \frac{1}{Rm} * \left[\left(\frac{b_{i+1,j}^k - b_{i-1,j}^k}{2\Delta r} \right) \right. \\ & \left. + \left(\frac{1}{r_{i,j}^k} \right) * \left(\frac{b_{i+1,j}^k - b_{i-1,j}^k}{2\Delta r} \right) + \left(\frac{b_{i,j+1}^k - 2b_{i,j}^k + b_{i,j-1}^k}{(\Delta z)^2} \right) \right] \end{aligned} \tag{20}$$

Equations 16-20 are the stencils for the momentum, energy, species concentration and magnetic equations having been reduced by finite difference method. The resulting systems of ordinary differential equations 16-20 alongside their boundary conditions expressed by equation 15 are simulated using MATLAB to obtain the profiles of the flow variables.

5. RESULTS AND DISCUSSIONS

Comprehensive numerical computations are calculated based on different flow parameters that characterizes the fluid flow and the results are expressed graphically as shown below. The accuracy of the numerical method and analysis is checked against the previously published results and an excellent agreement has been obtained in relation to the experimental analysis undertaken by Ibrahim et al. (2021) and Krishnendu et al. (2014). [3,4]

Figure 1

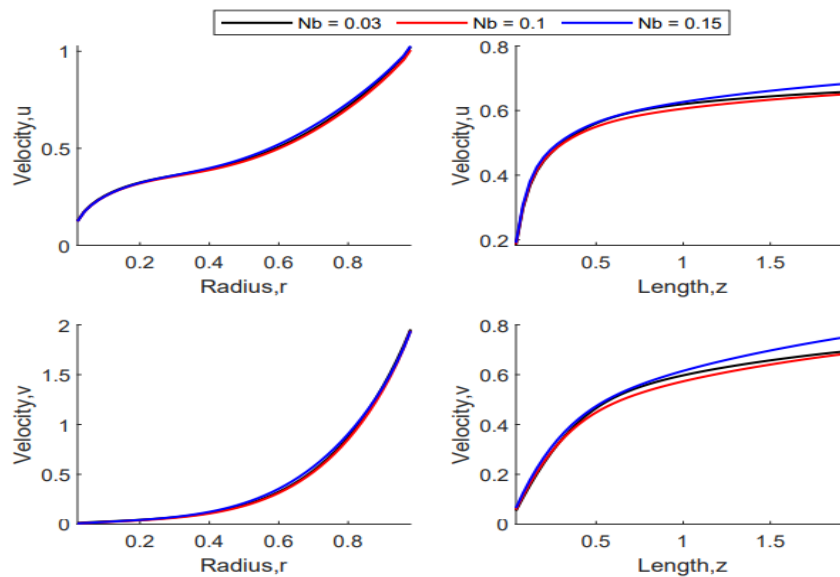


Figure 1 above depicts the effects of varying the Brownian motion parameter on the nanofluid flow velocity. From the diagram, an increase in the Brownian motion parameter tends to have minimal effect on the flow velocity.

Figure 2

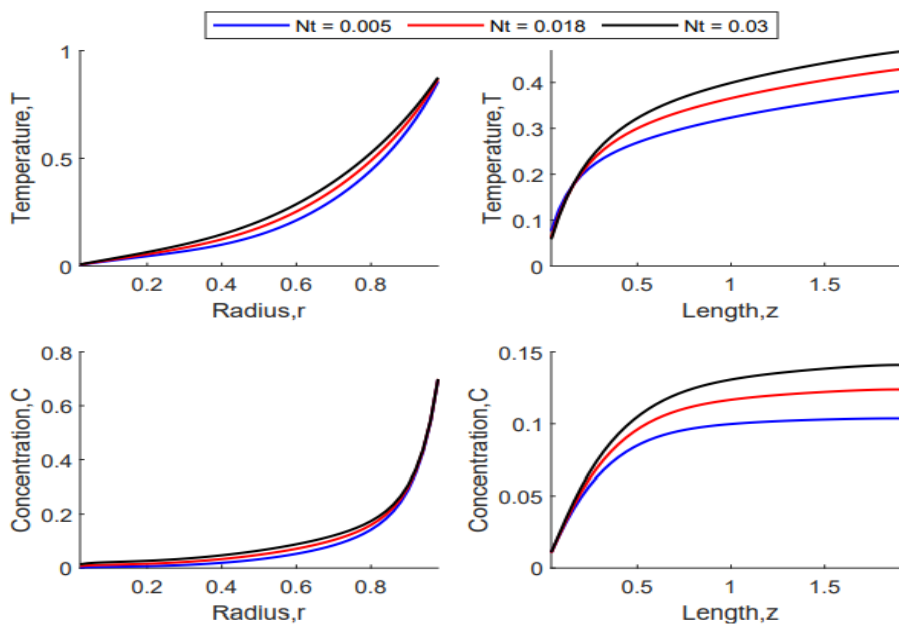


Figure 2 above presents the effects of the thermophoresis parameter Nt on the temperature distribution and nanoparticle concentration. With an increase in Nt , the temperature of the fluid increases. Equally, an increase in Nt results to an increase in the nanoparticle concentration. An increase in Nt results to an increase in the thermophoresis force which tends to move nanoparticles from the hot to cold region consequently increasing the magnitude of the temperature profiles and the nanoparticle concentration profiles. An increase in the thermophoresis parameter results to thickening of the nanoparticles concentration boundary layer. [5]

Figure 3

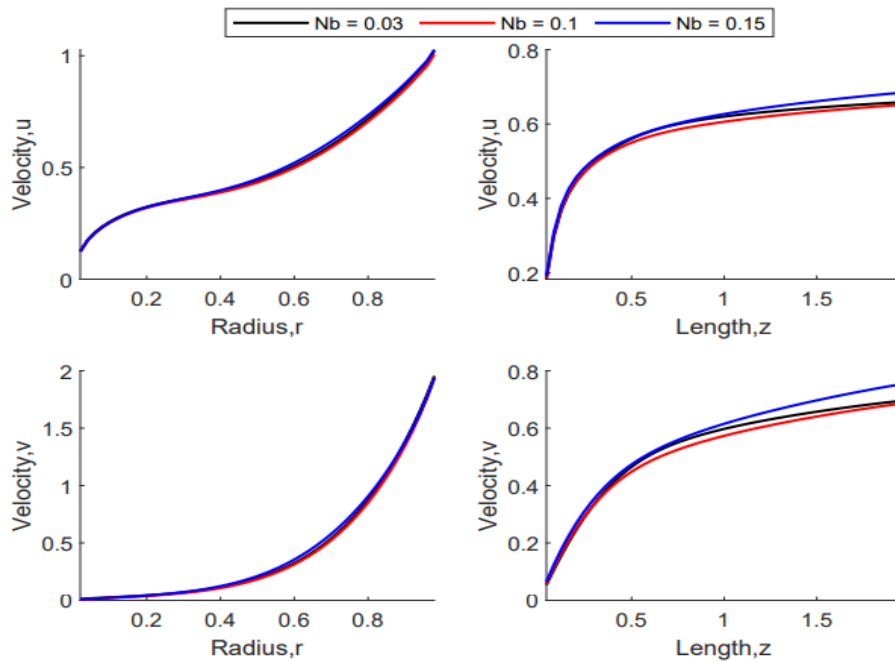


Figure 3 above displays the effects of varying the Brownian motion parameter Nb on the nanofluid velocity. From the figure, an increase in Nb results to a disruption in the flow velocity. This is attributed to the fact that an increase in Nb results to thermal fluctuations which disrupts the structure of the magnetic field in the fluid. Such disruptions leads to the formation of turbulent eddies which makes the flow velocity to be chaotic. [5]

Figure 4

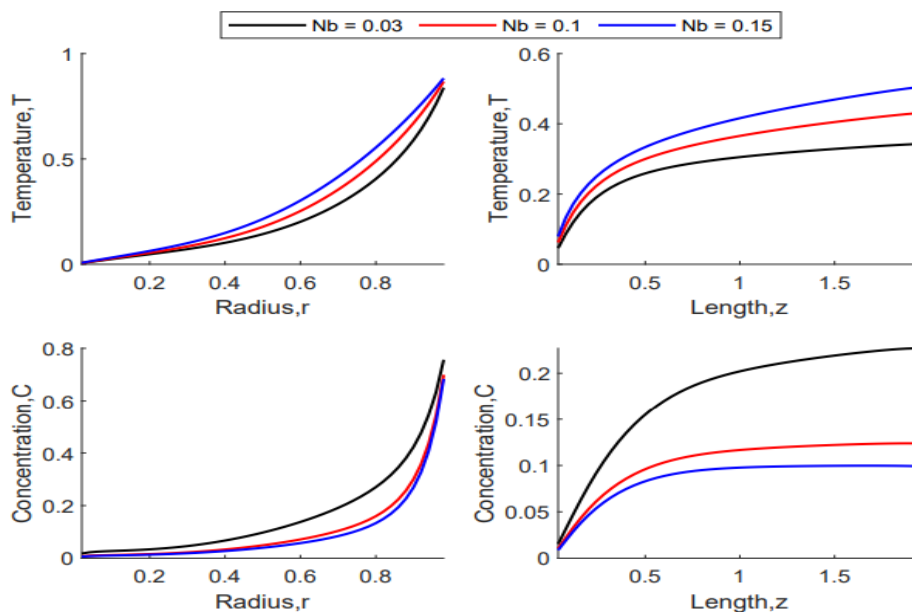


Figure (d): Effects of Brownian motion parameter Nb on the dimensionless temperature and the dimensionless nanoparticle concentration.

Figure 4 above depicts the effects of Brownian motion parameter Nb on the dimensionless temperature and the dimensionless nanoparticle concentration. The figure reveals that an increase in Brownian motion parameter results to an increase in the fluid temperature but the nanoparticle concentration decreases. This is because, the presence of the nanoparticles causes Brownian motion to take place and thus for an increase in Nb the Brownian motion is affected consequently affecting the heat transfer characteristic of the nanofluid. An increase in Nb causes the nanoparticle concentration boundary layer to diminish. [5]

Figure 5

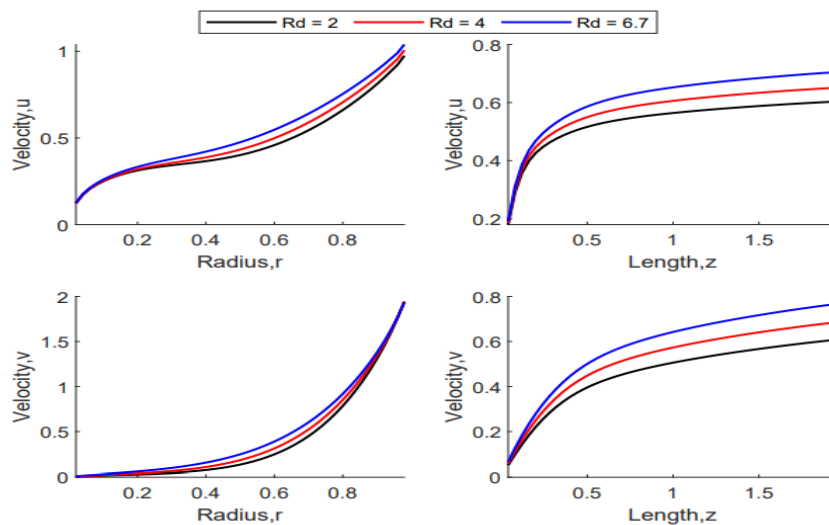


Figure 5 above depicts the effects of varying the radiation parameter Rd on the velocity of the nanofluid. From the figure, an increase in Rd results to an increase in both the radial and axial velocities. This is because, an increase in Rd enhances thermal convection thus resulting to an increase in the fluid velocity. The radiative heat transfer induces a temperature gradient in the fluid which causes the fluid to flow in a convective manner.

Figure 6

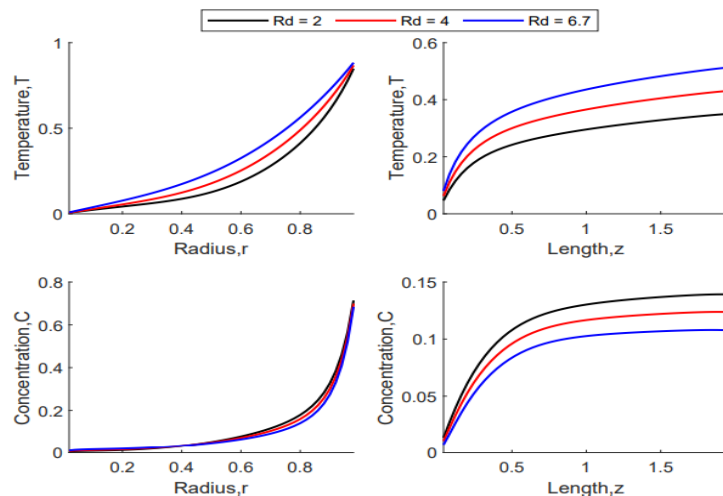


Figure 6 above shows the effect of varying the radiation parameter Rd on the temperature and concentration profiles of the nanofluid. From the figure, an increase in the radiation parameter Rd results to an increase in the fluid temperature but

results to a decrease in the nanoparticles concentration. Generally, an increase in the radiation parameter means the radiative heat transfer is more dominant in the flow as compared to the convective heat transfer. An increase in the radiation parameter impairs the mixing of the nanoparticles in the base fluid thus lowering the concentration of the nanofluid. The presence of thermal radiation increases the temperature of the fluid thus favoring heat transfer.

Figure 7

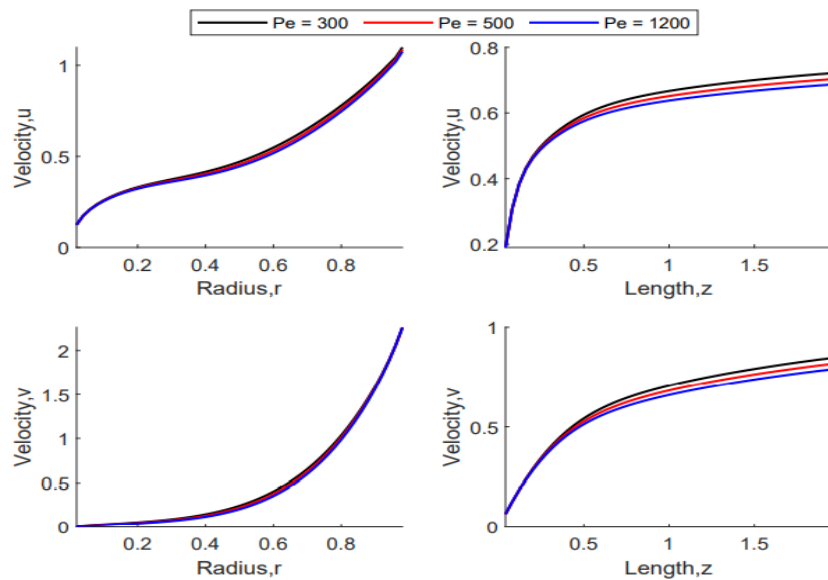


Figure 7 above presents the effect of varying the Peclet number Pe on the velocity profiles. The Peclet number is a dimensionless parameter that varies between the convective and diffusive heat transfer. Generally, an increase in the Peclet number favors the convective heat transfer to the diffusive heat transfer. Thus an increase in the Peclet number leads to an increase in the mixing of the nanoparticles in the base fluid which reduces the flow velocity of the nanofluid.

Figure 8

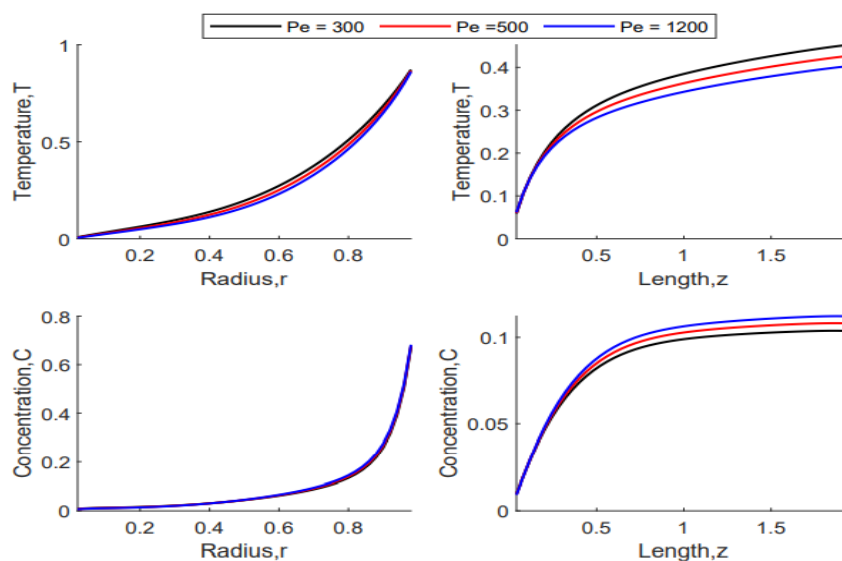


Figure 8 above presents the effect of varying the Peclet number Pe on the temperature and concentration profiles. From the figure, it is evident that an increase in the Peclet number results to a decrease in the fluid temperature but enhances the

nanoparticle concentration profile. Generally, an increase in the Peclet number favors convective heat transfer over diffusive heat transfer. This means convective heat transfer becomes more dominant as compared to the diffusive heat transfer. An increase in the Peclet number results to a more chaotic flow which in turn enhances the fluid particle mixing thus an increase in the concentration. The chaotic nature of the flow favors the convective heat transfer thus heat transfer at the surface-nanofluid boundary is negatively impacted resulting to a temperature drop.

6. CONCLUSION

The effects of Thermophoresis and Brownian motion parameter variation on heat and mass transfer on MHD nanofluid flow in a parabolic thermal solar collector was considered and researched. The results show that increasing the Thermophoresis (Nt) and Brownian motion parameters (Nb) lead to an increase in heat transfer and a decrease in mass transfer. Similarly, an increase in the Peclet number favors mass transfer but impairs heat transfer. Thermophoresis (Nt), Brownian motion parameters (Nb) and Peclet number have a significant impact on the MHD flow, and can be used to control the heat and mass transfer rates in MHD fluid flow by altering the parameters to achieve expected flow velocity that gives the required heat and mass transfer in an engineering process.

ACKNOWLEDGEMENTS

The author expresses his cordial gratitude to Dr. Kimathi and Dr. Muli of the Department of Mathematics of Machakos University, Kenya and the former Director of the Directorate of Criminal Investigations, Kenya Mr. George Kinoti, CBS for their encouragement and support during the undertaking of this research.

REFERENCES

- [1] Abdullah-Al-Mahbub, M., Islam, A., Almohamad, H., Al Dughairi, A., Al-Mutiry, M., & Abdo, H. (2022). Different Forms of Solar Energy Progress: The Fast-Growing Eco-Friendly Energy Source in Bangladesh for a Sustainable Future. *Energies* 2022, 15, 6790. Retrieved from <https://doi.org/10.3390/en15186790>.
- [2] R. Kandasamy, I. Muhaimin, Radiah Mohamad, Thermophoresis and Brownian motion effects on MHD boundary-layer flow of a nanofluid in the presence of thermal stratification due to solar radiation, *International Journal of Mechanical Sciences*, Volume 70, 2013, Pages 146-154, ISSN 0020-7403, <https://doi.org/10.1016/j.ijmecsci.2013.03.007>. (<https://www.sciencedirect.com/science/article/pii/S0020740313000829>)
- [3] JOUR Xu, Hang, Ibrahim, Wubshet, Tulu, Ayele, 2019. Magnetohydrodynamic (MHD) Boundary Layer Flow Past a Wedge with Heat Transfer and Viscous Effects of Nanofluid Embedded in Porous Media, 4507852, 2019, 1024-123X. <https://doi.org/10.1155/2019/4507852>, 10.1155/2019/4507852, *Mathematical Problems in Engineering*. Hindawi.
- [4] Ur Rehman F., and Nadeem, S., 2018, "Heat Transfer Analysis for Three-Dimensional Stagnation Point Flow of Water-Based Nanofluid Over an Exponentially Stretching Surface," *ASME J. Heat Transfer*, 140(5), p. 052401.
- [5] Mabood, F., Khan, W. A., and Ismail, A. I. M., 2015, "MHD Boundary Layer Flow and Heat Transfer of Nanofluids Over a Nonlinear Stretching Sheet: A Numerical Study," *J. Magn. Magn. Mater.*, 374, pp. 569–576.
- [6] Sheikholeslami, M., and Ganji, D. D., 2016, "Nanofluid Convective Heat Transfer Using Semi Analytical and Numerical Approaches: A Review," *J. Taiwan Inst. Chem. Eng.*, 65, pp. 43–77.
- [7] Noreen, S., 2016, "Effects of Joule Heating and Convective Boundary Conditions on Magnetohydrodynamic Peristaltic Flow of Couple-Stress Fluid," *ASME J. Heat Transfer*, 138(9), p. 094502.